Computational Mathematical Modelling of Radiative Chemical Reaction and Hall Effects on unsteady flow past an Isothermal Vertical Plate with radiation and Heat Absorption.

Dr. Sowgani Ramakrishna [a], Dr. Anumandla Srinivas [b], Dr. Nookala Venu*[c]

[a] Department of Mathematics, Balaji Institute of Technology and Science, Narsampet, Warangal- 506331, Telangana, India (UGC Autonomous Institute).
[b] Department of Mathematics, Balaji Institute of Technology and Science, Narsampet, Warangal- 506331, Telangana, India (UGC Autonomous Institute).
[c] * Department of Internet of Things (IoT), Madhav Institute of Technology & Science, Gwalior - 474005, Madhya Pradesh, India (A Govt. Aided UGC Autonomous Institute).
ramakrishnas5385@gmail.com, anumandlasrinivas8845@gmail.com,venunookala@mitsgwalior.in

Article History: **Received:** 02.06.2023 **Revised:**20.07.2023 **Accepted:** 01.08.2023

ABSTRACT

The influence of elasticity of flexible walls on peristaltic transport of a dusty fluid with heat and mass transfer in a horizontal channel in the presence of chemical reaction has been investigated under long wavelength approximation The effects of radiation, chemical reaction and porosity of the medium on unsteady flow of a viscous, incompressible and electrically conducting fluid past an exponentially accelerated vertical plate with variable wall temperature and mass diffusion in the presence of transversely applied uniform magnetic field. The plate temperature and the concentration level near the plate increase linearly with time. The fluid model under consideration has been solved by perturbation technique. The model contains equations of motion, diffusion equation and equation of energy. To analyze the solution of the model, reasonable sets of the values of the parameters have been considered. The effects of various parameters on heat and mass transfer characteristics of the flow are discussed through graphs.

Keywords: *Wall properties, Hall Current, Channel flow, Radiation, Chemical reaction, MHD, Mass Diffusion.*

[a] Department of Mathematics, Balaji Institute of Technology and Science, Narsampet, Warangal- 506331, Telangana, India (UGC Autonomous Institute).
[b] Department of Mathematics, Balaji Institute of Technology and Science, Narsampet, Warangal- 506331, Telangana, India (UGC Autonomous Institute).
[c] * Department of Internet of Things (IoT), Madhav Institute of Technology & Science, Gwalior - 474005, Madhya Pradesh, India (A Govt. Aided UGC Autonomous Institute).
ramakrishnas5385@gmail.com, anumandlasrinivas8845@gmail.com,venunookala@mitsgwalior.in

DOI: 10.48047/ecb/2023.12.8.685

1. INTRODUCTION

The physical mechanism of the flow induced by the travelling wave can be well understood and is known as the so-called peristaltic transport mechanism. Peristaltic pumping is also used in medical instruments such as the heart–lung machine [1]. Investigation on peristaltic transport of non-Newtonian fluids is of utmost importance owing to its wide range of applications in engineering and biology [2]. In particular, the study of such fluids has applications in a number of processes that occur in industry such as the extrusion of polymer fluids, solidification of liquid crystals, cooling of metallic plate in a bath, exotic lubricants, colloidal and suspension solutions. Investigation of hydro magnetic natural convection flow with heat and mass transfer in porous and non-porous media has drawn considerable attentions of several researchers owing to its applications in geophysics, astrophysics, aeronautics, meteorology, electronics, chemical, and metallurgy and petroleum industries. Magnetohydrodynamic (MHD) natural convection flow of an electrically conducting fluid with porous medium has also been successfully exploited in crystal formation [3]. However, thermal radiation effects on hydromagnetic natural convection flow with heat and mass transfer play a vital role in manufacturing processes viz. glass production, design of fins, steel rolling, furnace design, casting and levitation, etc. Moreover, several engineering processes occur at very high temperatures where the knowledge of radiative heat transfer becomes indispensible for the design of pertinent equipment. Nuclear power plants, gas turbines and various propulsion devices for missiles, aircraft, satellites and space vehicles are examples of such engineering areas [4]. The study of natural convection flow induced by the simultaneous action of thermal and solutal buoyancy forces acting over bodies with different geometries in a fluid with porous medium is prevalent in many natural phenomena and has varied a wide range of industrial applications [5]. For example, the presence of pure air or water is impossible because some foreign mass may be present either naturally or mixed with air or water due to industrial emissions, in atmospheric flows [6]. Natural processes such as attenuation of toxic waste in water bodies, vaporization of mist and fog, photosynthesis, transpiration, sea-wind formation, drying of porous solids, and formation of ocean currents occur due to thermal and solutal buoyancy forces developed as a result of difference in temperature or concentration or a combination of these two [7]. Such configuration is also encountered in several practical systems for industry based applications viz. cooling of molten metals, heat exchanger devices, petroleum reservoirs, insulation systems, filtration, nuclear waste repositories, chemical catalytic reactors and processes, desert coolers, frost formation in vertical channels, wet bulb thermometers, etc. Considering the importance of such fluid flow problems [8-12].

2. MATHEMATICAL FORMULATION

An unsteady hydromagnetic flow of fluid past an infinite isothermal vertical plate with varying mass diffusion exists. The fluid and the plate rotate in unison with a uniform angular velocity Ω' about the $z'-$ axis normal to the plate. Initially the fluid is assumed to be at rest and surrounds an infinite vertical plate with temperature T'_∞ and concentration C'_∞. A magnetic field of uniform strength B_0 is transversely applied to the plate. The $x'-$axis is taken along the plate in the vertically upward direction and the $z'-$axis is taken normal to the plate [13-21]. The physical model of the problem shown in fig. (1). At time $t'>0$, the plate and the fluid are at the same temperature T'_∞ in the stationary condition with concentration level C'_∞ at all the points. At time $t'>0$, the plate is subjected to a uniform velocity $u=u_0$ in its own plane against the gravitational force. The plate temperature

and concentration level near the plate are raised uniformly and are maintained constantly thereafter [22-26]. All the physical properties of the fluid are considered to be constant except the influence of the body force term. Then under the usual Boussinesq's approximation the unsteady flow equations are momentum equation, energy equation, and mass equation respectively [27-31].

Equation of Momentum:

$$\frac{\partial u'}{\partial t'} - 2\Omega' v = \nu \frac{\partial^2 u}{\partial z^2} - \frac{1}{\rho}\frac{\partial \rho}{\partial x} + g + \frac{B_0}{\rho} j_y \tag{1}$$

$$\frac{\partial v}{\partial t} - 2\ \Omega'\ u = \nu\ \frac{\partial^2 v}{\partial z^2} - \frac{B_0}{\rho}\ j_x \tag{2}$$

Equation of Energy

$$\rho c_p \frac{\partial T'}{\partial t'} = k \frac{\partial^2 T'}{\partial z^2} - \frac{\partial q}{\partial z} \tag{3}$$

Equation of diffusion

$$\frac{\partial C'}{\partial t'} = D \frac{\partial^2 C}{\partial z^2} - Kr'\left(C - C'_\infty\right) \tag{4}$$

As, no large velocity gradient here, the viscous term in equation (1) vanishes for small and hence for the outer flow, beside there is no magnetic field along $x-$ direction gradient [32-38]. So this results in,

$$0 = D\frac{\partial \rho}{\partial x} - p_\infty g \tag{5}$$

By eliminating the pressure term from equation (1) and (5), we obtain

$$\frac{\partial u'}{\partial t'} - 2\Omega' v = \nu \frac{\partial^2 u}{\partial z^2} - \frac{1}{\rho}\frac{\partial \rho}{\partial x} + \left(\rho_\infty - \rho\right) g + \frac{B_0}{\rho} j_y \tag{6}$$

The Boussinesq approximation gives

$$\rho_\infty - \rho = \rho_\infty \beta\left(T' - T'_\infty\right) + \rho_\infty \beta\left(C' - C'_\infty\right) \tag{7}$$

On using (2.7) in the equation (2.6) and noting that ρ_∞ is approximately equal to 1, the momentum equation reduces to

$$\frac{\partial u'}{\partial t'} - 2\Omega' v = \nu \frac{\partial^2 u}{\partial z^2} + \frac{B_0}{\rho} j_y + g\ \beta\left(T' - T'_\infty\right) + g\ \beta^*\left(C' - C'_\infty\right) \tag{8}$$

The generalized Ohm's law with Hall currents is taken into account and ion – slip and thermo-electric

$$j + \frac{\omega \mathrm{T}_e}{B_0}\left(j \times B\right) = \sigma\left[E + q \times B\right] \tag{9}$$

The equation (9) gives

$$j_x - mj_y = \sigma v B_0 \tag{10}$$

$$j_y - mj_x = \sigma u B_0 \tag{11}$$

where $m = \omega_e \mathrm{T}_e$ is Hall parameter.

Solving (10) and (11) for j_x and j_y, we have

$$j_x = \frac{\sigma B_0}{\left(1+m^2\right)}\left(v - mu\right) \tag{12}$$

$$j_y = \frac{\sigma B_0}{\left(1+m^2\right)}\left(u - mv\right) \tag{13}$$

where B_0 – Imposed magnetic field, m – Hall parameter, ν – Kinematic viscosity, Ω_z – Component of angular viscosity, Ω – Non-dimensional angular velocity, J_z – component of current density j, ρ – Fluid density, σ – Electrical conductivity, t' – Time, μ – Coefficient of viscosity, T – Temperature of the fluid near the plate, T_w – Temperature of the plate, θ – Dimensionless temperature, T_∞ – Temperature of the fluid far away from the plate, C – Dimensionless concentration, κ – Thermal conductivity, β – Volumetric coefficient of thermal expansion, β^* – Volumetric coefficient of expansion with concentration, C' – Species concentration in the fluid, C_w – Wall concentration, C_∞ – Concentration for away from the plate, t – Non-dimensional time $\left(u, v, w\right)$ – Components of velocity field F, $\left(U, V, W\right)$ – Non dimensional velocity components, $\left(x, y, z\right)$ – Cartesian co-ordinates [39-42].

On the use of (12) and (13), the momentum equations (8) and (2) become

$$\frac{\partial u'}{\partial t'} = \nu \frac{\partial^2 u}{\partial z^2} + 2\Omega' v - \frac{\sigma \mu_e^2 H_0^2}{\rho\left(1+m^2\right)}\left(u + mv\right) + g\ \beta\left(T' - T'_\infty\right) + g\ \beta^*\left(C' - C'_\infty\right) \tag{14}$$

$$\frac{\partial v}{\partial t'} = \nu \frac{\partial^2 u}{\partial z^2} + 2\Omega v - \frac{\sigma \mu_e^2 H_0^2}{\rho\left(1+m^2\right)}\left(v - mu\right) \tag{15}$$

$$\rho C_p \frac{\partial T}{\partial t'} = k \frac{\partial^2 T}{\partial z^2} - \frac{\partial q}{\partial z} \tag{16}$$

$$\frac{\partial C'}{\partial t'} = D \frac{\partial^2 C'}{\partial z^2} - Kr'\left(C - C'_\infty\right) \tag{17}$$

Due to small Coriolis force, the second term on the right side of the equation (14) and (15) comes into existence [43-52].

The boundary conditions are given by:

$$\begin{aligned} &u = 0, \quad T = T_\infty^*, \;\; C = C_\infty^*, \qquad\qquad \forall \;\; y, t' \le 0 \\ t' > 0 :\; &u = u_0, T \to T_w, C' = C_\infty' + \left(C_w' - C_\infty'\right) \quad at \quad y = 0 \\ &u \to 0, T \to T_\infty, C' \to C_\infty' \qquad\qquad at \quad y \to \infty \end{aligned}$$

$$u = 0, \quad T = T, \;\; C = C_\infty, \; v = 0 \qquad \forall \;\; y, t' \le 0 \tag{18}$$

$$u \to u, T \to T_w, C' = C_w', v = 0 \quad at \quad z = 0 \;\; for \;\; all \; t' \le 0 \tag{19}$$

The dimensionless quantities are introduced as follows:

$$\begin{aligned} &U = \frac{u}{u_0}, V = \frac{v}{u_0}, t = \frac{t' u_0^2}{\nu}, Z = \frac{z u_0^2}{\nu^2}, \Omega = \Omega \frac{\nu}{u_0^2}, M^2 = \frac{\sigma \mu_e^2 {H_0}^2 \nu}{2 \rho {u_0}^2}, \Pr = \frac{\mu c_p}{\kappa} \\ &Gr = \frac{g \beta \nu \left(T_\omega - T_\infty\right)}{{u_0}^3}, Gc = \frac{g \beta^* \nu \left(C_\omega' - C_\infty'\right)}{{u_0}^3}, R = \frac{16 a^* \sigma \nu^2 T_\infty^3}{k u_0^2}, Kr = \frac{Kr' \nu}{u_0^2} \end{aligned} \tag{20}$$

where $Sc-$ Schmidt number, $Gr-$Thermal Grashof number, $Gc-$Mass Grashof number, $\Pr-$ Prandtl number, $M-$ Hartman number, $Kr-$Chemical reaction parameter, $R-$Radiation parameter [53-59]. Together with the equation (1), (2), (3) and (4), boundary conditions (18), (19), using (20), we have

$$\frac{\partial U}{\partial t} = \frac{\partial^2 U}{\partial Z^2} + 2V\left(\Omega - \frac{2m^2}{1+m^2}\right) + \frac{2m^2}{1+m^2} U + Gr \;\; \theta + Gc \;\; C \tag{21}$$

$$\frac{\partial V}{\partial t} = \frac{\partial^2 V}{\partial Z^2} - 2U\left(\Omega + \frac{2m^2}{1+m^2}\right) + \frac{2m^2}{1+m^2} \; V \tag{22}$$

The boundary conditions

$$\begin{aligned} &U = 0, \;\; \theta = 0, \;\; C = 0, \;\; V = 0 \qquad \forall \;\; Z, t \le 0 \\ &U \to 1, \;\; \theta \to 1, \;\; C \to t, \;\; V \to 0 \qquad \forall \qquad t > 0 \end{aligned} \tag{23}$$

$$U \to 0, \;\; \theta \to 0, \;\; C \to 0, \;\; V \to 0 \qquad \forall \qquad t > 0 \tag{24}$$

Now equations (21), (22) and the boundary conditions (23), (24) can be combined to give:

$$\frac{\partial F}{\partial t} = \frac{\partial^2 F}{\partial Z^2} - F \;\; a + Gr \;\; \theta + Gc \;\; C \tag{25}$$

$$\frac{\partial \theta}{\partial t} = \frac{1}{\Pr} \frac{\partial^2 \theta}{\partial Z^2} - \frac{R}{\Pr} \; \theta \tag{26}$$

$$\frac{\partial C}{\partial t} = \frac{1}{Sc} \frac{\partial^2 C}{\partial Z^2} - Kr \;\; C \tag{27}$$

where $F = U + iV$ and $a = 2\left[\frac{M^2}{\left(1+m^2\right)} + i\left(\Omega - \frac{M^2 m}{\left(1+m^2\right)}\right)\right]$

In this study the value of (rotation parameter) is taken to be $\Omega - \frac{M^2 m}{\left(1+m^2\right)}$, as a result of this the transverse velocity vanishes with the boundary conditions

$$\begin{aligned} &F = 0,\ \ \theta = 0,\ \ C = 0 && \forall\ \ Z, t \le 0 \\ &F \to 1,\ \ \theta \to 1,\ \ C \to t,\ \ \ at\ Z = 0 && \forall\ \ \ t > 0 \\ &F \to 0,\ \ \theta \to 0,\ \ C \to 0,\ \ \ at\ Z \to \infty && \forall\ \ \ t > 0 \end{aligned} \tag{28}$$

3. METHOD OF SOLUTION

Equation (25) – (27) are coupled, non – linear partial differential equations and these cannot be solved in closed – form using the initial and boundary conditions (28). However, these equations can be reduced to a set of ordinary differential equations, which can be solved analytically [60-69]. This can be done by representing the velocity, temperature and concentration of the fluid in the neighborhood of the fluid in the neighborhood of the plate as

$$\begin{aligned} F\left(z,t\right) &= F_0\left(z\right)e^{i\omega t} \\ \theta\left(z,t\right) &= \theta_0\left(z\right)e^{i\omega t} \\ C\left(z,t\right) &= C_0\left(z\right)e^{i\omega t} \end{aligned} \tag{29}$$

Substituting (29) in Equation (25) – (27) and equating the harmonic and non – harmonic terms, we obtain

$$F_0'' - \beta_3^2 F_0 = -Gr\,\theta_0 - GmC_0 \tag{30}$$

$$\theta_0'' - \beta_2^2 \theta_0 = 0 \tag{31}$$

$$C_0'' - \beta_1^2 Sc\, C_0 = 0 \tag{32}$$

The corresponding boundary conditions can be written as

$$\begin{aligned} &F_0 = 1,\ \theta_0 = 1,\ \ C_0 = t, && at\ Z = 0 \\ &F_0 = 0,\ \ \theta_0 = 0, C_0 = 0, && as\ Z \to \infty \end{aligned} \tag{33}$$

Solving the equations (30) – (32) under the boundary condition (33), we get the solution for fluid velocity; temperature; concentration is expressed below using perturbation method:

$$F_0 = A_1 e^{-\beta_2 y} + A_2 e^{-\beta_1 y} + A_3 e^{\beta_3 y}$$

$$\theta_0 = e^{-\beta_2 y}$$

$$C_0 = t\ e^{-\beta_1 y}$$

In view of the above equation (29) becomes

$$F\left(z,t\right) = \left\{A_1 e^{-\beta_2 y} + A_2 e^{-\beta_1 y} + A_3 e^{\beta_3 y}\right\} e^{i\omega t}$$

$$\theta\left(z,t\right) = \left\{e^{-\beta_2 y}\right\} e^{i\omega t}$$

$$C\left(z,t\right) = \left\{t\ e^{-\beta_1 y}\right\} e^{i\omega t}$$

Coefficient of Skin-Friction

The coefficient of skin-friction at the vertical porous surface is given by

$$C_f = \left(\frac{\partial F}{\partial Z}\right)_{z=0} = -\left(\beta_2 A_1 + \beta_1 A_2 + \beta_3 A_3\right)$$

Coefficient of Heat Transfer

The rate of heat transfer in terms of Nusselt number at the vertical porous surface is given by

$$Nu = \left(\frac{\partial T}{\partial Z}\right)_{z=0} = -\beta_2$$

Sherwood number

$$Sh = \left(\frac{\partial C}{\partial Z}\right)_{Z=0} = t\ \beta_1$$

4. RESULTS AND DISCUSSIONS

The problem has been formulated, analyzed and solved analytically using perturbation technique. The effect of parameters like thermal Grashof number (Gr), mass Grashof number (Gc), Schmidt number (Sc), Reaction parameter (K), Chemical reaction parameter (Kr), Radiation Parameter (R), Prandtl number (Pr), Hartmann number (M), Hall parameter (m) on Axial Velocity (F), Temperature (θ) and Concentration (C) are computed and intercepted through graphs.

The effects of Grashof numbers for heat and mass transfer (Gr, Gc) are illustrated in Fig. (2) respectively. The Grashof number for heat transfer signifies the relative effect of the thermal buoyancy force to the viscous hydrodynamic force in the boundary layer. As expected, it is observed that there was a rise in the axial velocity due to the enhancement of thermal buoyancy force. Also, as (Gr) increases, the peak values of the velocity increases rapidly near the porous plate and then decays smoothly to the free stream velocity. The Grashof number for mass transfer (Gc) defines the ratio of the species buoyancy force to the viscous hydrodynamic force. As expected, the fluid velocity increases and the peak value is more distinctive due to increase in the species buoyancy force. The velocity distribution attains a distinctive maximum value in the vicinity of the plate and then decreases properly to approach the free stream value. It is noticed that the velocity increases with increasing values of the Grashof number for mass transfer. The influences of the Schmidt number (Sc) on the axial velocity profiles are plotted in Fig. (3) respectively. It is noticed from this figure that, the axial velocity decrease on increasing Sc. The Schmidt number embodies the ratio of the momentum to the mass diffusivity. The Schmidt number therefore quantifies the relative effectiveness of momentum and mass transport by diffusion in the

hydrodynamic (velocity) boundary layer. Fig. (4) display the effect of magnetic field parameter or Hartmann number (M) on axial velocity. It is seen from these figures that the axial velocity increases when M increases. That is the axial velocity fluid motion is retarded due to application of transverse magnetic field. This phenomenon clearly agrees with the fact that Lorentz force that appears due to interaction of the magnetic field and fluid axial velocity resists the fluid motion. The influence of the hall parameter (m) on axial velocity profiles is as shown in Figs. (5) respectively. It is observed from these figures that the axial velocity profiles increase with an increase in the hall parameter m. This is because, in general, the Hall currents reduce the resistance offered by the Lorentz force. This means that Hall currents have a tendency to increase the fluid velocity components. Fig. (6) Illustrates the behaviour of axial velocity profiles for different values of the chemical reaction parameter (Kr) . It is pertinent to mention that $(Kr > 0)$ corresponds to a destructive chemical reaction. It can be seen from the profiles that the axial velocity increases in the degenerating chemical reaction in the boundary layer. This is due to the fact that the increase in the rate of chemical reaction rate leads to thinning of a momentum in a boundary layer in degenerating chemical reaction. It can be seen from the profiles that the cross flow axial velocity reduces in the degenerating chemical reaction. It is evident from Fig. (7) that, the thermal radiation parameter (R) leads to increases in the axial velocity with increasing values of thermal radiation parameter. Thus, the Fig. (7) are in excellent agreement with the laws of Physics. Thus as R increases, the axial velocity increases. Now, from this figure, it may be inferred that radiation has a more significant effect on temperature than on velocity. Thus, the thermal radiation does not have a significant effect on the velocities but produces a comparatively more pronounced effect on the temperature of the mixture. It is noticed form Fig. (8) that the effects of rotation on the axial respectively. It is evident from Fig. (8) that, axial velocity increases on increasing in reaction parameter (K) .This implies that rotation retards fluid flow in the axial velocity flow direction and accelerates fluid flow in the axial velocity flow direction in the boundary layer region. This may be attributed to the fact that when the frictional layer at the moving plate is suddenly set into the motion then the Coriolis force acts as a constraint in the main fluid flow. Fig. (9) Shows the temperature profile for different values of Prandtl number (Pr). It is observed that temperature increases with decrease in values of Prandtl number and also heat transfer is predominant in air when compared to water. Fig. (10) indicates that effect of radiation parameter (R) on the temperature profiles. It is deduced that temperature profiles decrease of the fluid near the plate decrease when radiation parameter are increased. Physically, thermal radiation causes a fall in temperature of the fluid medium and thereby causes a fall in kinetic energy of the fluid particles. This results in a corresponding decrease in fluid velocities. Fig. (11) shows a destructive type of chemical reaction because the concentration decreases for increasing chemical reaction parameter which indicates that the diffusion rates can be tremendously changed by a chemical reaction. This is due to the fact that an increase in the chemical reaction Kr causes the concentration at the boundary layer to become thinner, which decreases the concentration of the diffusing species. This decrease in the concentration of the diffusing species diminishes the mass diffusion. Fig. (12) represents the concentration profile for various values of Schmidt number (Sc). It is noticed that the concentration field decreases with increase in values of Schmidt number.

Appendix

$$\beta_1^2 = (i\omega + Kr)Sc,\ \beta_2^2 = (R + i\omega \Pr),\ \beta_3^2 = (i\omega + a),\ A_1 = -\frac{Gr}{\beta_2^2 - \beta_3^2},\ A_2 = -\frac{Gr\ t}{\beta_1^2 - \beta_3^2}$$

REFERENCES

[1] Vaigandla, K. K., & Venu, D. N. (2021). A survey on future generation wireless communications-5G: multiple access techniques, physical layer security, beamforming approach. *Journal of Information and Computational Science*, *11*(9), 449-474.

[2] Venu, D., Arun Kumar, A., & Vaigandla, K. K. (2022). Review of Internet of Things (IoT) for Future Generation Wireless Communications. *International Journal for Modern Trends in Science and Technology*, *8*(03), 01-08.

[3] Sujith, A. V. L. N., Swathi, R., Venkatasubramanian, R., Venu, N., Hemalatha, S., George, T., & Osman, S. M. (2022). Integrating nanomaterial and high-performance fuzzy-based machine learning approach for green energy conversion. *Journal of Nanomaterials*, *2022*, 1-11.

[4] Venu, N., & Anuradha, B. (2013, December). Integration of hyperbolic tangent and Gaussian kernels for fuzzy C-means algorithm with spatial information for MRI segmentation. In *2013 Fifth International Conference on Advanced Computing (ICoAC)* (pp. 280-285). IEEE.

[5] Vaigandla, K. K., & Venu, D. N. (2021). Ber, snr and papr analysis of ofdma and sc-fdma. GIS Science Journal, ISSN, (1869-9391), 970-977.

[6] Venu, N. (2014, April). Performance and evalution of Guassian kernals for FCM algorithm with mean filtering based denoising for MRI segmentation. In *2014 International Conference on Communication and Signal Processing* (pp. 1680-1685). IEEE.

[7] Karthik Kumar Vaigandla, D. (2021, November). Survey on Massive MIMO: Technology, Challenges, Opportunities and Benefits. *YMER* , 271-282.

[8] Venu, N., & Anuradha, B. (2015). Multi-Kernels Integration for FCM algorithm for Medical Image Segmentation Using Histogram Analysis. *Indian Journal of Science and Technology*, *8*(34), 1-8.

[9] Venu, N., Yuvaraj, D., Barnabas Paul Glady, J., Pattnaik, O., Singh, G., Singh, M., & Adigo, A. G. (2022). Execution of Multitarget Node Selection Scheme for Target Position Alteration Monitoring in MANET. *Wireless Communications and Mobile Computing*, *2022*.

[10] Venu, N., Swathi, R., Sarangi, S. K., Subashini, V., Arulkumar, D., Ralhan, S., & Debtera, B. (2022). Optimization of Hello Message Broadcasting Prediction Model for Stability Analysis. *Wireless Communications & Mobile Computing (Online)*, *2022*.

[11] Venu, D. N. (2015). Analysis of Xtrinsic Sense MEMS Sensors. *International Journal of Advanced Research in Electrical, Electronics and Instrumentation Engineering* , *4* (8), 7228-7234.

[12] Venu, N., & Anuradha, B. (2013). A novel multiple-kernel based fuzzy c-means algorithm with spatial information for medical image segmentation. *International Journal of Image Processing (IJIP)*, *7*(3), 286.

[13] Nookala Venu, A. (2018). Local mesh patterns for medical image segmentation. *Asian Pacific Journal of Health Sciences*, *5*(1), 123-127.

[14] Venu, N., & Anuradha, B. (2013). PSNR Based Fuzzy Clustering Algorithms for MRI Medical Image Segmentation. *International Journal of Image Processing and Visual Communication*, *2*(2), 01-07.

[15] Thouti, S., Venu, N., Rinku, D. R., Arora, A., & Rajeswaran, N. (2022). Investigation on identify the multiple issues in IoT devices using Convolutional Neural Network. *Measurement: Sensors*, *24*, 100509.

[16] Venu, N., Revanesh, M., Supriya, M., Talawar, M. B., Asha, A., Isaac, L. D., & Ferede, A. W. (2022). Energy Auditing and Broken Path Identification for Routing in Large-Scale Mobile Networks Using Machine Learning. *Wireless Communications and Mobile Computing*, *2022*.

[17] Nookala Venu, B. A. (2015). Medical Image Segmentation Using Kernal Based Fuzzy C-Means Algorithm. *International Journal of Engineering Innovation & Research* , *4* (1), 207-212.

[18] Nookala Venu, D., Kumar, A., & Rao, M. A. S. (2022). BOTNET Attacks Detection in Internet of Things Using Machine Learning. *Neuroquantology*, *20*(4), 743-754.

[19] Venu, N., & Anuradha, B. (2014, February). Multi-Hyperbolic Tangent Fuzzy C-means Algorithm for MRI Segmentation. In *Proceedings of International Conference on Advances in Communication, Network and Computing (CNC-2014), Elsevier* (pp. 22-24).

[20] Nookala Venu, S. W. (2022). A Wearable Medicines Recognition System using Deep Learning for People with Visual Impairment. *IJFANS*, *12*(1), 2340-2348.

[21] Nookala Venu, G. R. (2022). Smart Road Safety and Vehicle Accidents Prevention System for Mountain Road. *International Journal for Innovative Engineering Management and Research , 11* (06), 209-214.

[22] Nookala Venu, D., Kumar, A., & Rao, M. A. S. (2022). Smart Agriculture with Internet of Things and Unmanned Aerial Vehicles. *Neuroquantology*, *20*(6), 9904-9914.

[23] Nookala Venu, D., Kumar, A., & Rao, M. A. S. (2022). Internet of Things Based Pulse Oximeter For Health Monitoring System. *NeuroQuantology*, *20*(5), 5056-5066.

[24] Venu, D. N. DA (2021). Comparison of Traditional Method with watershed threshold segmentation Technique. *The International journal of analytical and experimental modal analysis*, *13*, 181-187.

[25] Dr.Nookala Venu, D. K. (2022). Investigation on Internet of Things (IoT):Technologies, Challenges and Applications in Healthcare. *International Journal of Research , XI* (II), 208-218.

[26] Mr.RadhaKrishna Karne, M. M. (2022). Applications of IoT on Intrusion Detection System with Deep Learning Analysis. *International Jourfor Innovative Engineering and Management Research , 11* (06), 227-232.

[27] Venu, N., & Anuradha, B. (2015). Two different multi-kernels for fuzzy C-means algorithm for medical image segmentation. *Int. J. Eng. Trends Technol.(IJETT)*, *20*, 77-82.

[28] Dr. Nookala Venu, D. A. (2022, March). Routing and Self-Directed Vehicle Data Collection for Minimizing Data Loss in Underwater Network. *IJFANS International Journal of Food and Nutritional Sciences* , 170-183.

[29] Dr. Nookala Venu, D. A. (2022). Fuzzy Based Resource Management Approach for the Selection of Biomass Material. *IJFANS International Journal of Food and Nutritional Sciences , 12* (2), 83-97.

[30] Ravindra Kumar Agarwal, D. S. (2022). A Novel Dates Palm Processing and Packaging Management System based on IoT and Deep Learning Approaches. *IJFANS International Journal of Food and Nutritional Sciences , 11* (8), 1139-1151.

[31] Manthur Sreeramulu Manjunath, P. K. (2022). An Enhanced Machine Learning Approach For Identifying Paddy Crop Blast Disease Management Using Fuzzy Logic. *IJFANS International Journal of Food and Nutritional Sciences , 11* (8), 1152-1163.

[32] K.P.Senthilkumar, K. C. (2022). Machine Learning Based Analysis and Classification of Rhizome Rot Disease in Turmeric Plants. *IJFANS International Journal of Food and Nutritional Sciences , 11* (8), 1179-1190.

[33] Sowmya Jagadeesan, B. B. (2022). A Perishable Food Monitoring Model Based on IoT and Deep Learning to Improve Food Hygiene and Safety Management. *IJFANS International Journal of Food and Nutritional Sciences , 11* (8), 1164-1178.

[34] Nookala Venu, S. K. (2022). Machine Learning Application for Medicine Distribution Management System. *IJFANS International Journal of Food and Nutritional Sciences , 11* (1), 2323-2330.

[35] Reddy, A. V., Kumar, A. A., Venu, N., & Reddy, R. V. K. (2022). On optimization efficiency of scalability and availability of cloud-based software services using scale rate limiting algorithm. *Measurement: Sensors*, *24*, 100468.

[36] Venu, D. N. (2022). Smart Agriculture Remote Monitoring System Using Low Power IOT Network. *IJFANS International Journal of Food and Nutritional Sciences , 11* (6), 327-340.

[37] Venu, D. N. (2022). IOT Surveillance Robot Using ESP-32 Wi-Fi CAM & Arduino. *IJFANS International Journal of Food and Nutritional Sciences , 11* (5), 198-205.

[38] Nookala Venu, N. S. (2022). Study and Experimental Analysis on FBMC and OFDM. *International Journal for Innovative Engineering and Management Research , 11* (6), 49-53.

[39] Sandhya rani B, S. K. (2022). Vehicle Fuel Level Monitor and Locate the Nearest Petrol Pumps using IoT. *International Journal for Innovative Engineering and Management Research , 11* (06), 233-240.

[40] Nookala Venu, K. A. (2022). Face Mask Detection System Using Python Open CV, *International Journal for Innovative Engineering and Management Research, 11* (6), 28-32.

[41] Nookala Venu, V. M. (2022). Alcohol Detection and Engine Locking System. *International Journal for Innovative Engineering and Management Research , 11* (06), 157-160.

[42] Nookala Venu, C. B. (2022). Wireless Night Vision Camera on War Spying Robot. *International Journal for Innovative Engineering and Management Research , 11* (06), 123-128.

[43] Venu, D. N. (2022). IOT Based Enabled Parking System in Public Areas. *IJFANS International Journal of Food and Nutritional Sciences, 11* (4), 162-174.

[44] Venu, D. N. (2022). IOT Based Speech Recognition System to Improve the Performance of Emotion Detection. *IJFANS International Journal of Food and Nutritional Sciences, 11* (3), 92-102.

[45] Dr.Nookala Venu, M. S. (2018). Local Maximum Edge Binary Patterns for Medical Image Segmentation. *International Journal of Engineering and Techniques, 4* (1), 504-509.

[46] Venu, N., & Anuradha, B. (2016). Multi-hyperbolic tangent fuzzy c-means algorithm with spatial information for MRI segmentation. *International Journal of Signal and Imaging Systems Engineering*, *9*(3), 135-145.

[47] Venu, N., & Anuradha, B. (2015). Hyperbolic Tangent Fuzzy C-Means Algorithm with Spatial Information for MRI Segmentation. *International Journal of Applied Engineering Research*, *10*(7), 18241-18257.

[48] Venu, N., & Anuradha, B. (2015, April). Two different multi-kernels integration with spatial information in fuzzy C-means algorithm for medical image segmentation. In *2015 International Conference on Communications and Signal Processing (ICCSP)* (pp. 0020-0025). IEEE.

[49] Nookala Venu, B. (2015). MRI Image Segmentation Using Gaussian Kernel Based Fuzzy C-Means Algorithm. *International Journal of Electronics Communication and Computer Engineering , 6* (1), 140-145.

[50] Venu, N., & Anuradha, B. (2015). Evaluation of Integrated Hyperbolic Tangent and Gaussian Kernels Functions for Medical Image Segmentation. *International Journal of Applied Engineering Research*, *10*(18), 38684-38689.

[51] Sowmya Jagadeesan, M. K. (2022). Implementation of an Internet of Things and Machine learning Based Smart Medicine Assistive System for Patients with Memory Impairment. *IJFANS International Journal of Food and Nutritional Sciences* , 1191-1202.

[52] Venu, D. N. (2023). Design Analysis and Classification of Digital Transmission Based Composite Relay and Artificial Neural Network Approach. *IJFANS International Journal of Food and Nutritional Sciences , 12* (1), 680-63.

[53] Venu, D. N. (2023). Biomass Studies on Pyrolysis of Sugarcane Bagasse and Cashew Nut Shell for Liquid Fuels. *IJFANS International Journal of Food and Nutritional Sciences , 11* (1), 695-706.

[54] Venu, D. N. (2023). Synthesis and Study on Feasibility of Ethanol Production from Leachate of Pretreatment of Sugarcane Bagasse. *IJFANS International Journal of Food and Nutritional Sciences , 12* (1), 707-715.

[55] Venu, D. N. (2022). Design and Performance Analysis of Super Critical Fluid Extraction for SC-CO2. *IJFANS International Journal of Food and Nutritional Sciences , 11* (12), 3854-3865.

[56] Venu, D. N. (2022). Supercritical Fluid Evaluation and Extraction of Phenol from Sugarcane Bagasse Pyrolysis Oil. *IJFANS International Journal of Food and Nutritional Sciences , 11* (12), 3866-3876.

[57] Sandhya rani, D. V. (2022). IOT Based Smart Irrigation System Using Node MCU. *International Journal For Innovative Engineering and Management Research , 11* (6), 100-106.

[58] Dr.Nookala Venu, A. E. (2022). Low Power Area Efficient ALU with Low Power Full Adder. *International Journal For Innovative Engineering and Management Research , 11* (06), 167-170.

[59] Nookala Venu, B.Anuradha"Brain MRI Medical Image Segmentation Using Fuzzy Based Clustering Algorithms", *International Journal of Engineering Trends and Technology (IJETT),* V22 (2), 83-88 April 2015. ISSN: 2231-5381. www.ijettjournal.org. published by seventh sense research group.

[60] Dr. Nookala Venu, D. K. (2023). Implementation of Hello Time Gaps Tracking Scheme for Network Stability Analysis in MANET. *European Chemical Bulletin , 12* (8), 5011-5026.

[61] Venu, D. N. (2022). Classification Analysis for Local Mesh Patterns Using Medical Image Segmentation. *IJFANS International Journal of Food and Nutritional Sciences , 11* (12), 5232-5241.

[62] Venu, D. N. (2022). PSNR Based Levels Evaluation of FCM Algorithm with Peak and Valley Filtering Based Brain Images. *IJFANS International Journal of Food and Nutritional Sciences*, 11 (12), 5242-5253.

[63] Venu, D. N. (2023). Segmentation Analysis for Local Maximum Edge Binary Patterns using Medical Images. *IJFANS International Journal of Food and Nutritional Sciences,* 12 (1), 917-927.

[64] Venu, D. N. (2023). PSNR Based Evalution of Spatial Guassian Kernals For FCM Algorithm with Mean and Median Filtering Based Denoising for MRI Segmentation. *IJFANS International Journal of Food and Nutritional Sciences*, 12 (1), 928-939.

[65] Venu, D. N. (2022). Multi Guassian Kernals for FCM Algorithm with Mean and Peak-Valley-Kernal Filtering Based Denoising for MRI Segmentation Using PSNR Analysis. *IJFANS International Journal of Food and Nutritional Sciences*, 11 (11), 1965-1976.

[66] Dr.A.Arun Kumar, D. N. (2023). Enhanced Security Packet Acceptance for Target Position Alteration using Multi Accepter Scheme Assigning Algorithm in MANET. *European Chemical Bulletin , 12* (8), 7003-7018.

[67] Dr.A.Arun Kumar, D. N. (2023). Analysis and Enhancement of Energy Auditing Routing for Identification of Broken Paths in Mobile Adhoc Networks . *European Chemical Bulletin , 12* (8), 7019-7034.

[68] Anita Tuljappa, V. N. (2022). Dufour and Chemical Reaction Effects on Two Dimensional incompressible flow of a Viscous fluid over Moving vertical surface. *NeuroQuantology* , 63-74.

[69] Ch. Achi Reddy, V. N. (2022). Magnetic Field And Chemical Reaction Effects on Unsteady Flow Past A Stimulate Isothermal Infinite Vertical Plate. *NeuroQuantology , 20* (16), 5360- 5373.

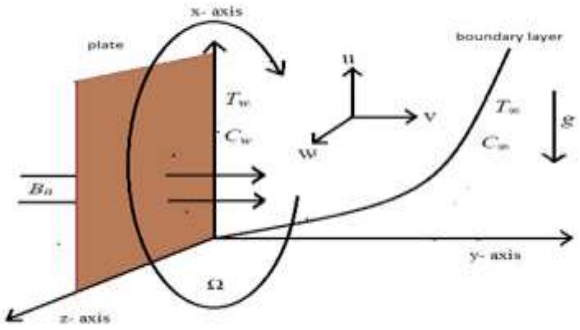

Fig. (1): The geometrical model of the problem

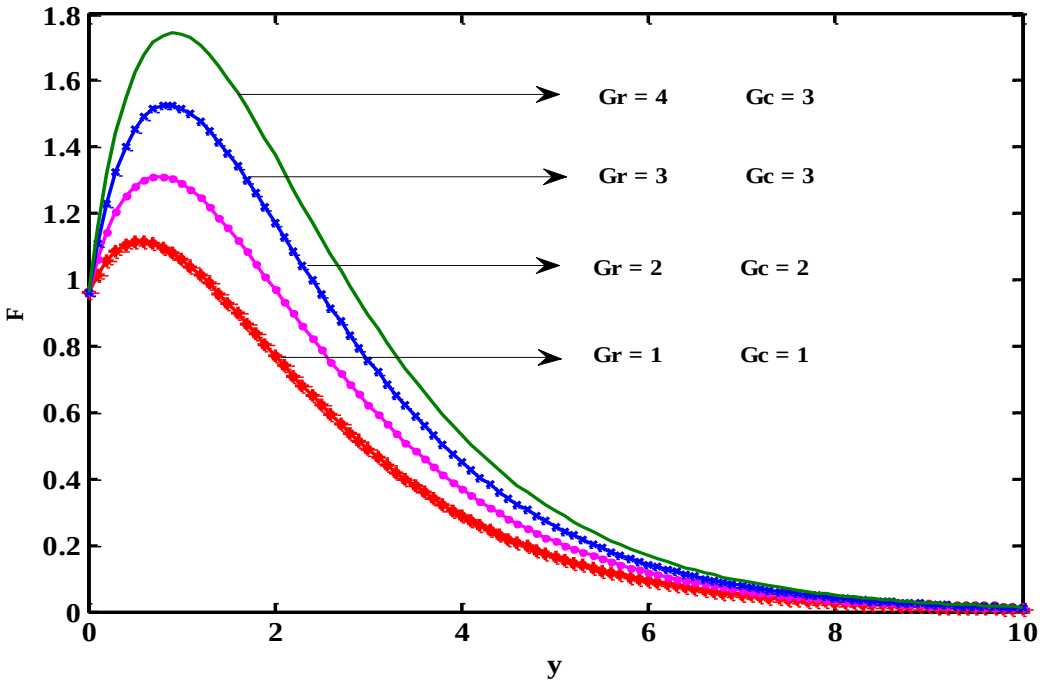

Fig. (2): Axial velocity profiles for different values of Gr, Gc

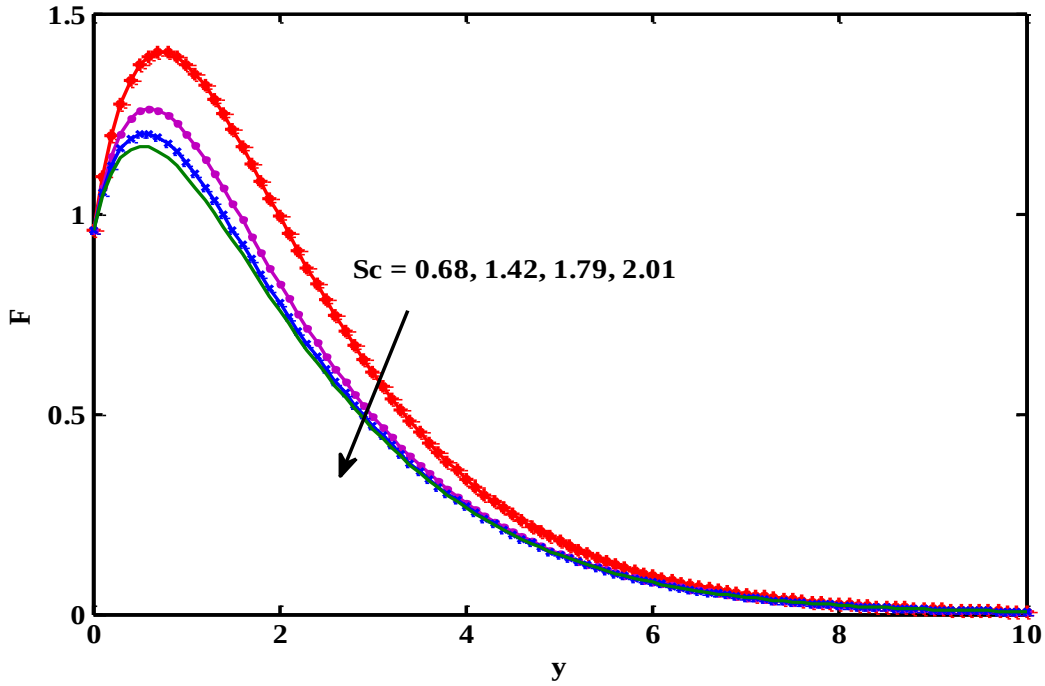

Fig. (3): Axial velocity profiles for different values of Sc

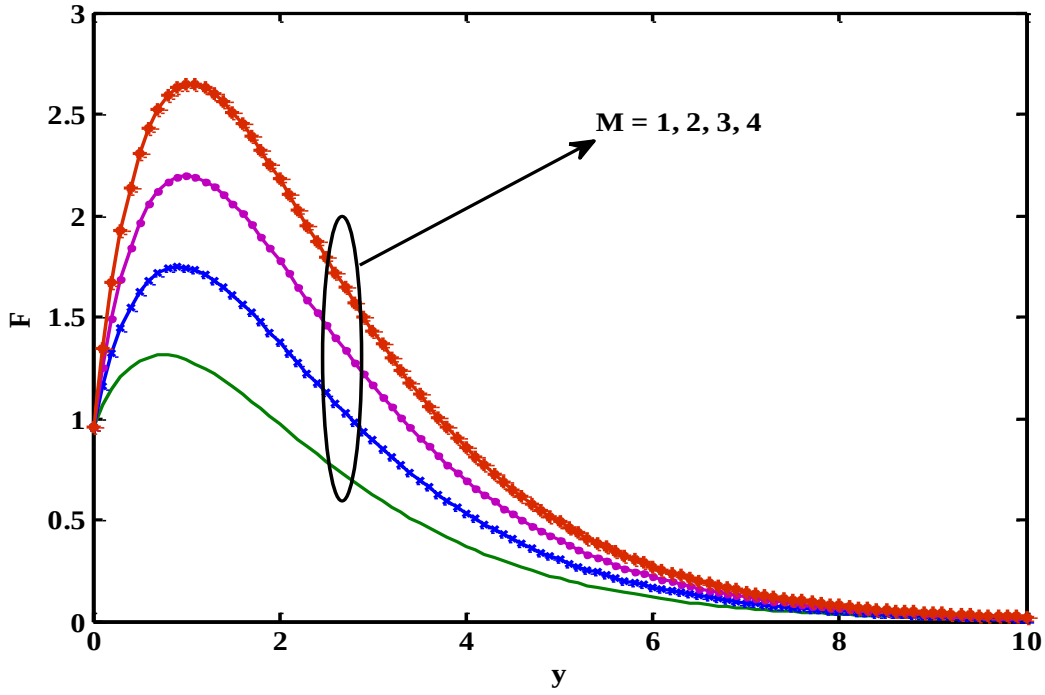

Fig. (4): Axial velocity profiles for different values of M

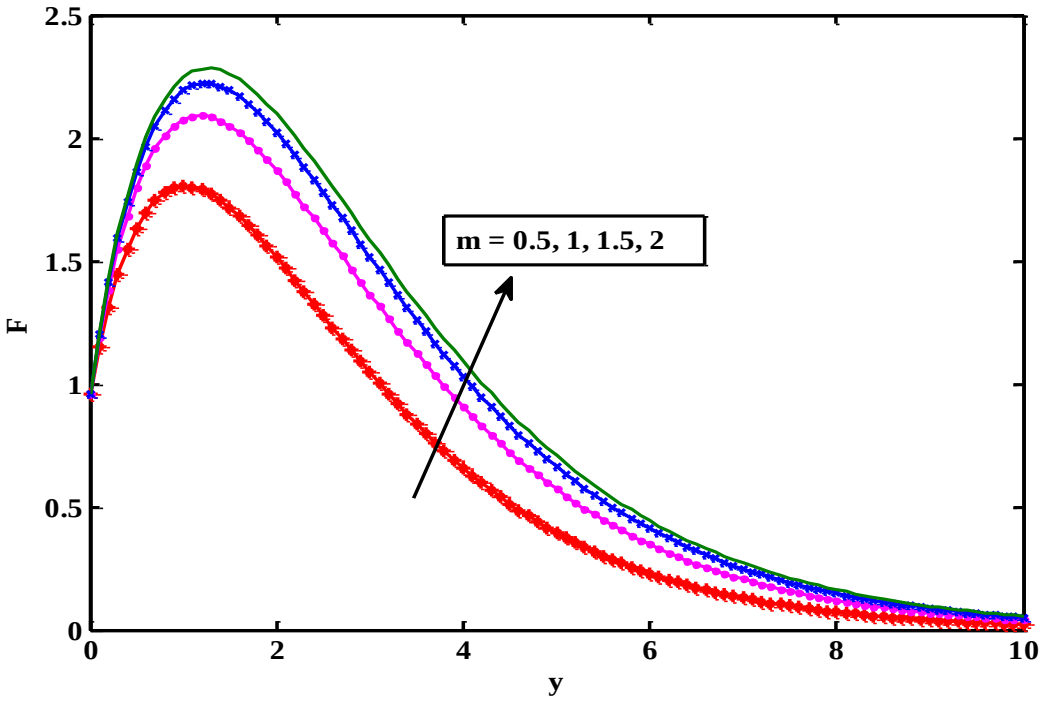

Fig. (5): Axial velocity profiles for different values of m

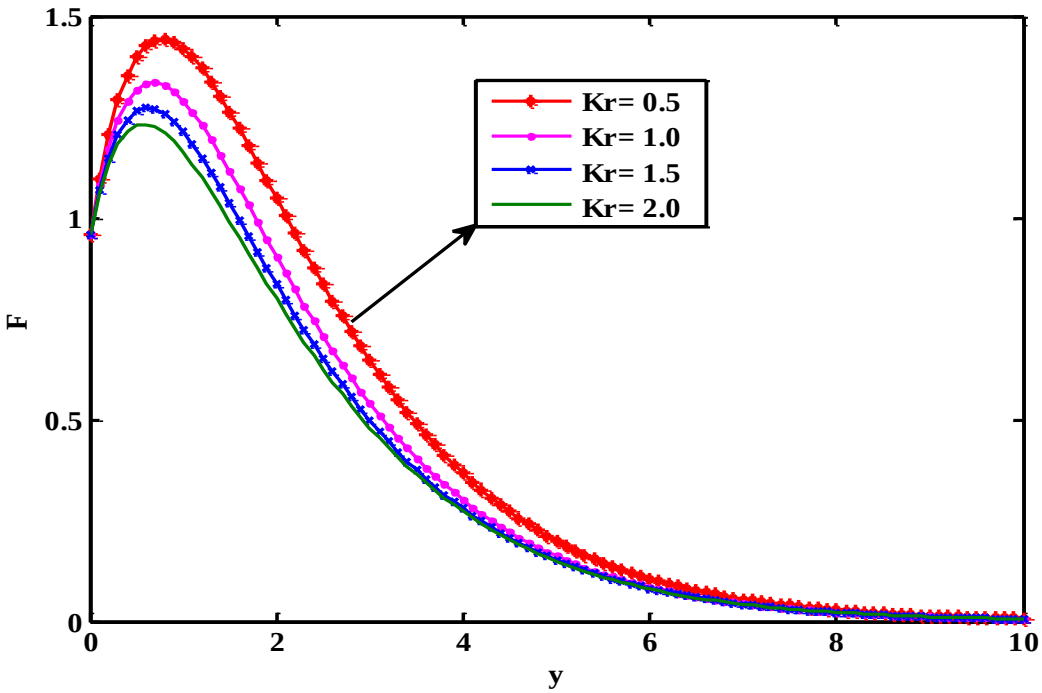

Fig. (6): Axial velocity profiles for different values of Kr

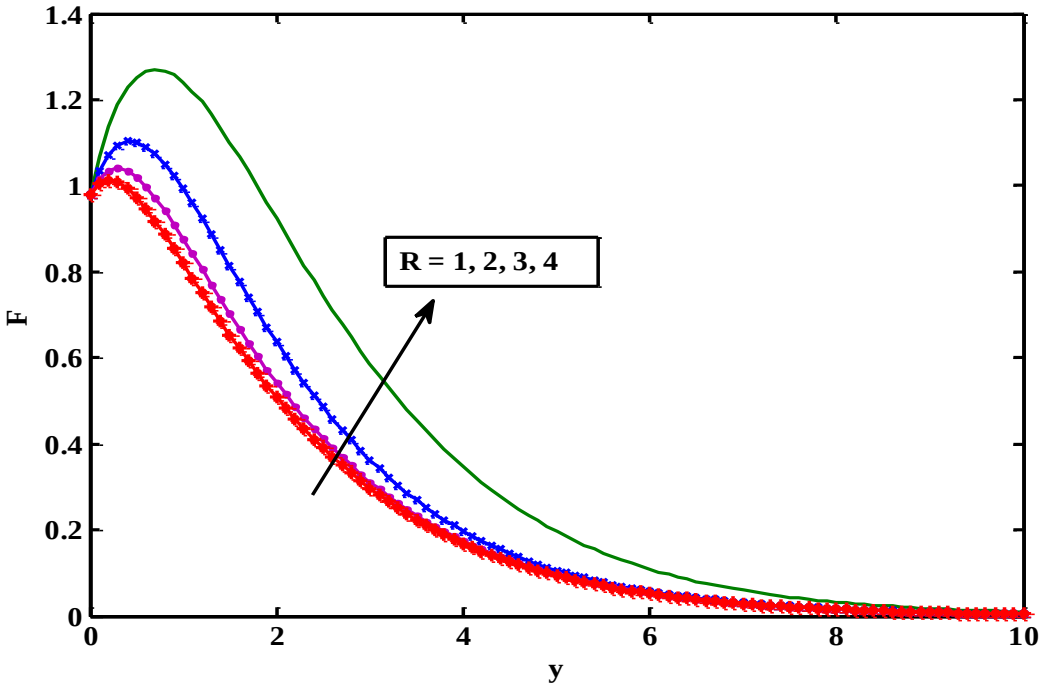

Fig. (7): Axial velocity profiles for different values of R

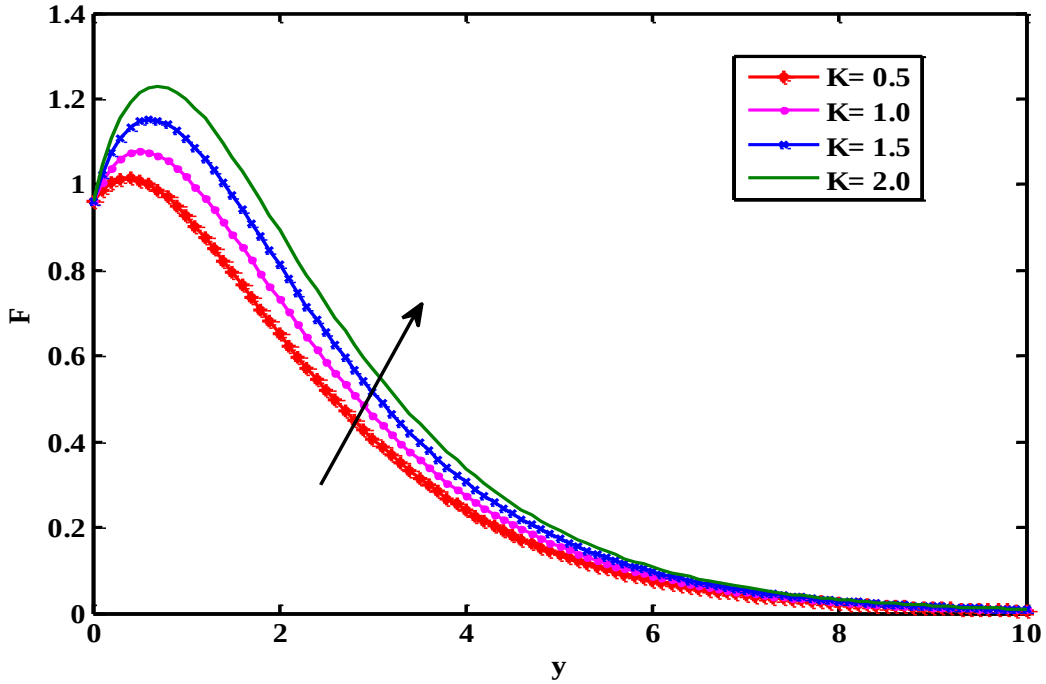

Fig. (8): Axial velocity profiles for different values of K

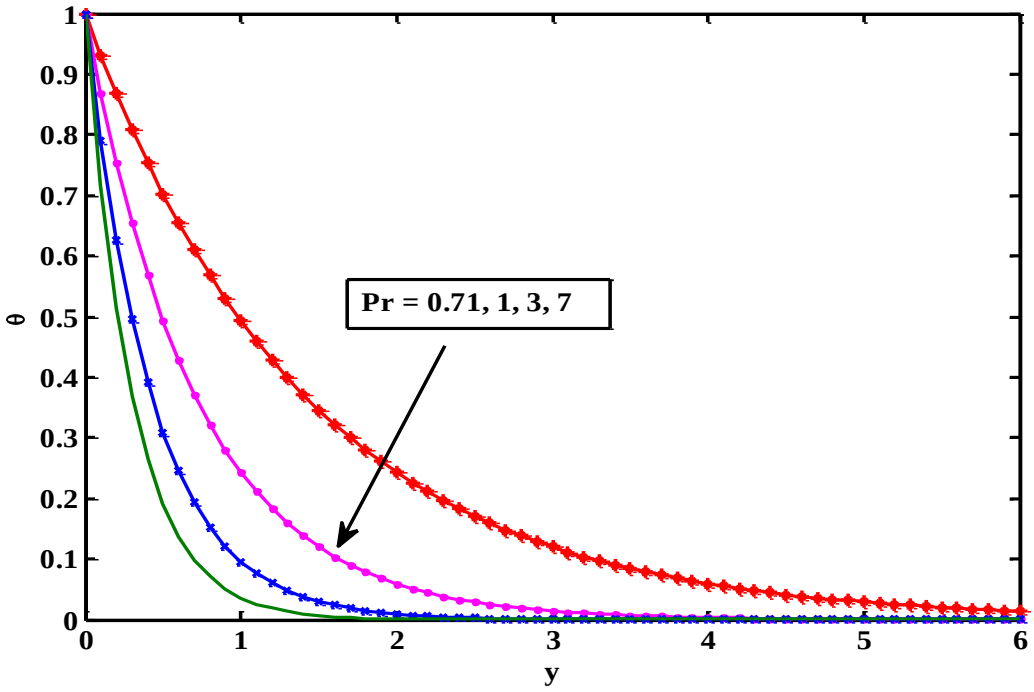

Fig. (9): Temperature profiles for different values of Pr

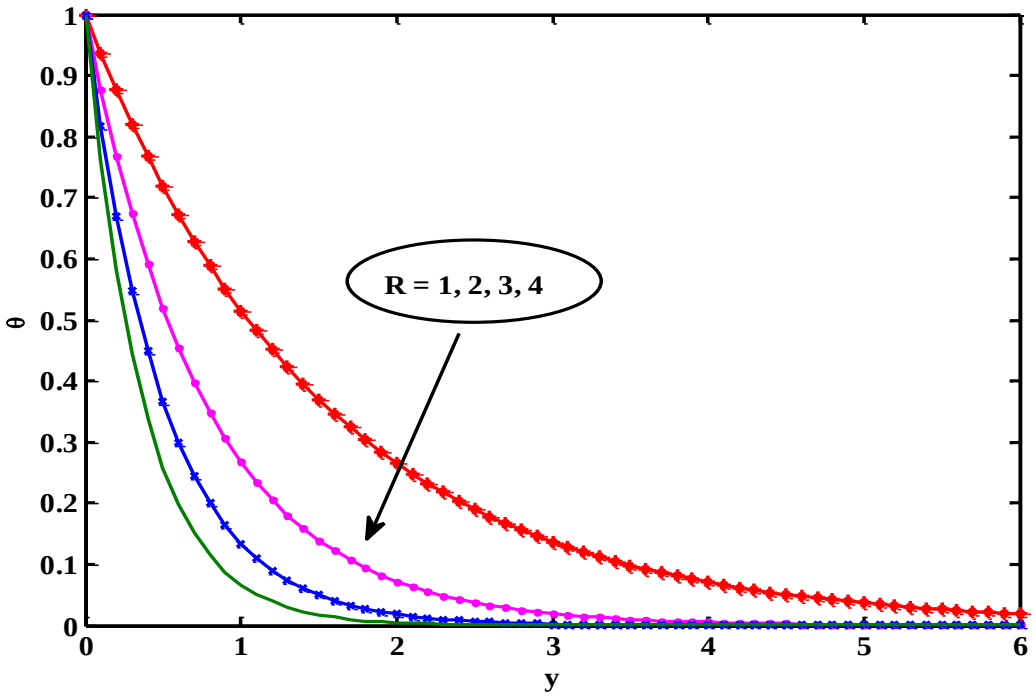

Fig. (10): Temperature profiles for different values of R

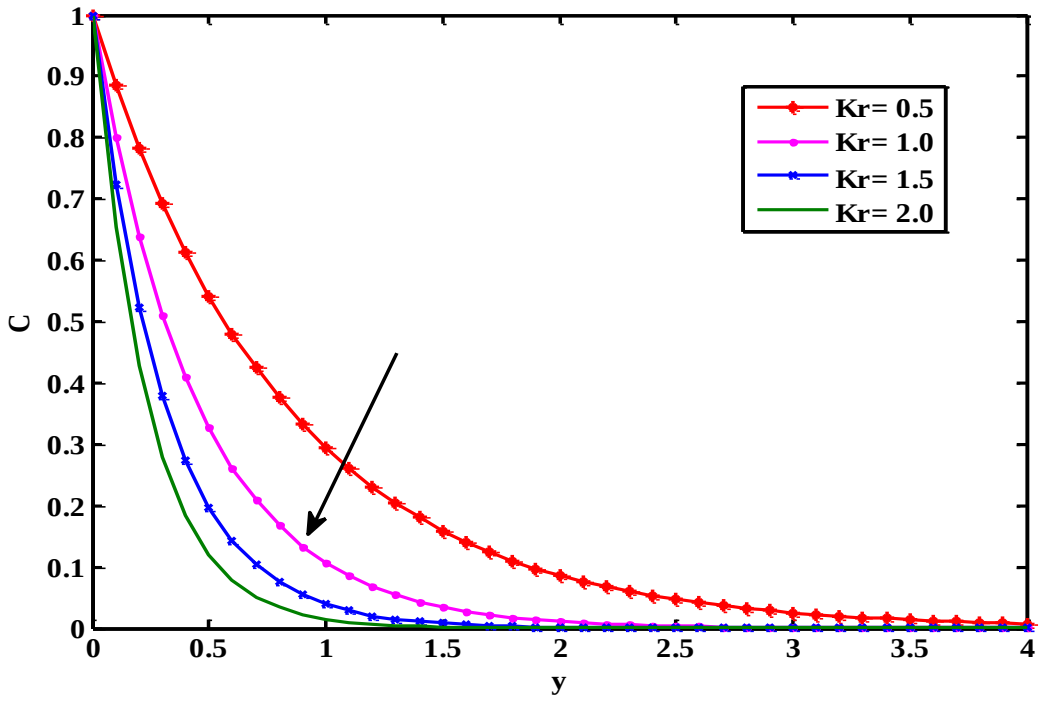

Fig. (11): Concentration profiles for different values of Kr

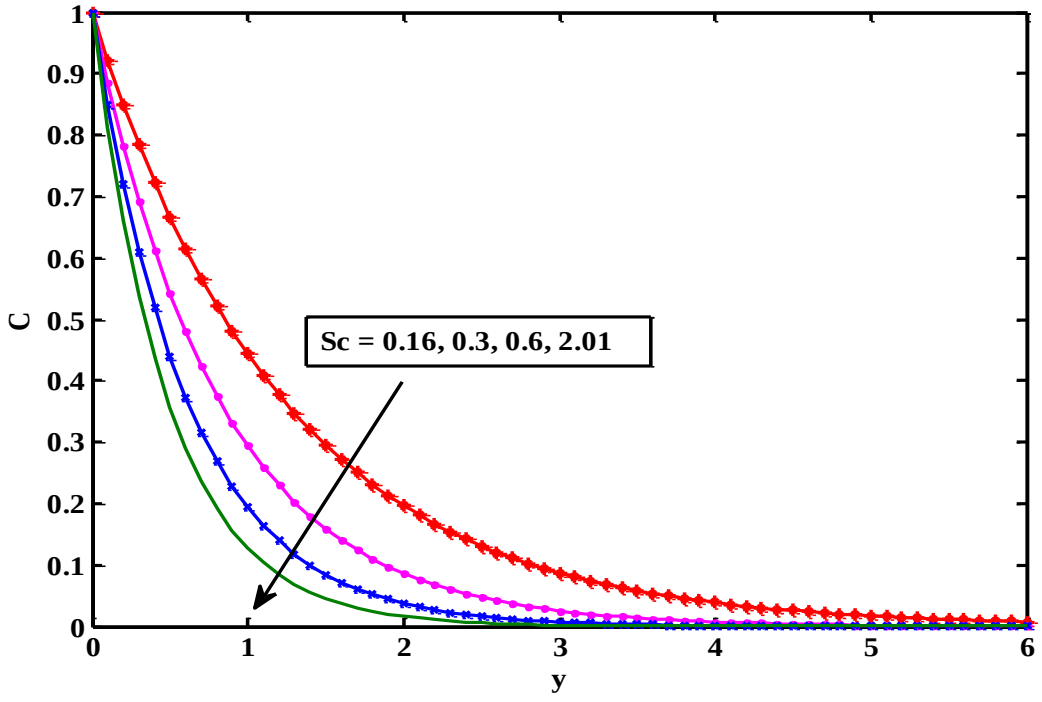

Fig. (12): Concentration profiles for different values of Sc